

In vitro analysis of the role of tumor necrosis factor-stimulated gene-6 in keloid

XINYI LI*, ZHAO CHEN*, XIAOJING LI and HUI WANG

Department of Plastic Surgery, The First Affiliated Hospital of Anhui Medical University, Hefei, Anhui 230022, P.R. China

Received June 21, 2018; Accepted November 8, 2018

DOI: 10.3892/mmr.2018.9767

Abstract. An increasing number of studies have demonstrated that tumor necrosis factor-stimulated gene-6 (TSG-6) has a key role in the progression of fibrosis; however, the exact effects of TSG-6 in keloid fibroblasts (KFs) remain unknown. The aim of the current study was to investigate the role of TSG-6 in the pathogenesis of keloids. Primary fibroblasts from 10 patients with keloid were cultured and transfected with pLVX-Puro or pLVX-Puro-TSG-6. Alterations of TSG-6 expression were then determined by reverse transcription-polymerase chain reaction (RT-PCR) and regulation was observed in KFs transfected with pLVX-Puro-TSG-6. Compared with the control group, transfection with pLVX-Puro-TSG-6 induced growth suppression, cell apoptosis and G2/M arrest in KFs. In addition, the mitochondrial apoptosis pathway was activated in KFs transfected with pLVX-Puro-TSG-6. These findings indicate that TSG-6 is a novel regulator of keloid fibrogenesis, and thus could be used/targeted TSG-6 as a promising treatment for keloid.

Introduction

A keloid is defined as an overgrowth of pathological scar tissue that grows beyond the original boundaries of the wound, does not regress spontaneously and tends to recur despite treatment (1,2). It can also spread to the surrounding skin by invasion (3). The clinical feature of keloid is a raised growth, usually accompanied by pain and pruritus (4). Since the mechanism and etiopathogenesis of keloids remain unknown, keloid therapy is very limited.

Tumor necrosis factor-stimulated gene-6 (TSG-6) was identified in differential screening of a cDNA library collected

from tumor necrosis factor-treated human diploid FS-4 fibroblasts (5). Multiple functions of TSG-6 have been proposed, including interacting with matrix-associated molecules or acting as an inflammatory factor (6,7). However, current knowledge on the physiological function of TSG-6 remains limited. It has been reported to be critical in maintaining the physiological architecture of skin (8). Furthermore, TSG-6 has potent anti-inflammatory properties, which have been investigated in several disease models, such as rheumatoid arthritis (9,10). In our previous rabbit ear model of hypertrophic scarring, injection of TSG-6 protein into the wound resulted in reduced hypertrophic scar formation and anti-inflammatory effects during wound healing (11). However, the role of TSG-6 in keloid remains unclear.

In the current study, a TSG-6 expression vector was constructed and stably transfected into human keloid fibroblasts (KFs). The effects of overexpression of TSG-6 on proliferation and apoptosis in KFs were determined. In addition, the potential mechanisms of the signaling pathway regulated via TSG-6 in KFs were investigated.

Materials and methods

Ethics. The current study was approved by the institutional review board of Anhui Medical University (Hefei, China), and written informed consent was obtained from all patients prior to inclusion. The study was performed according to the principles of the Declaration of Helsinki.

Keloid fibroblasts and cell culture. Ten patients were recruited from the First Affiliated Hospital of Anhui Medical University. The characteristics of participants with keloid in this study are listed in Table I. Patients had received no previous treatment for keloid. KFs were isolated and cultured as previously described (12). Cells were cultured in Dulbecco's modified Eagle's medium (DMEM), L-glutamine, 100 µg/ml streptomycin, 100 U/ml penicillin and fetal calf serum (Gibco; Thermo Fisher Scientific, Inc., Waltham, MA, USA). No morphological and biochemical differences were found with the passage.

Lentiviral vector construction and packaging. Total RNA was extracted from KFs using TRIzol reagent (Invitrogen; Thermo Fisher Scientific, Inc.) according to the manufacturer's instructions. cDNA synthesis was conducted according to the RNA

Correspondence to: Professor Xiaojing Li, Department of Plastic Surgery, The First Affiliated Hospital of Anhui Medical University, 210 Ji Xi Road, Shu Shan Hefei, Anhui 230022, P.R. China
E-mail: lixiaojing_anhui@hotmail.com

*Contributed equally

Key words: tumor necrosis factor-stimulated gene-6, apoptosis, proliferation, keloid, fibrosis

polymerase chain reaction (PCR) kit protocol (Takara Bio, Inc., Otsu, Japan). The TSG-6 cDNA (GenBank no. AJ421518) was amplified by PCR (Takara Bio, Inc.) from KF cDNA using the following oligonucleotide primers: Forward, 5'-GGAATT CATGATCATCTTAATTTACT-3'; and reverse, 5'-CGGGAT CCTAAGTGGCTAAATCTTCC-3'. The cycling for PCR amplifying reaction was: Reverse transcription (RT) 50°C, 5 min for 1 cycle; RT inaction 95°C, 20 sec for 1 cycle; denaturing 95°C, 15 sec for 40 cycles; annealing 60°C, 60 sec for 40 cycles. Sequencing results were analyzed using Basic Local Alignment Search Tool (BLAST) from National Center for Biotechnology Information (Bethesda, MD, USA). The amplified DNA was digested by the enzymes *EcoRI* and *BamHI* and ligated into lentiviral plasmid pLVX-Puro (Clontech Laboratories, Inc., Mountain View, CA, USA). Following transduction of DH5 α -competent *E. coli*, the positive clones were selected for PCR identification and DNA sequencing. Clones containing the target plasmids were selected and named pLVX-Puro-TSG-6.

pLVX-Puro-TSG-6 was highly purified and extracted with endotoxin-free solution. pLVX-Puro-TSG-6 was then co-transfected into 293T cells (Clontech Laboratories, Inc.) with pHelper 1.0 (Biovector Science Lab, Inc., Beijing, China) and pHelper 2.0 (Biovector Science Lab, Inc.) and lentiviruses using Lipofectamine[®] 2000 (Thermo Fisher Scientific, Inc.), according to the manufacturer's instructions. The 293T cells were cultured using Minimum Essential Media (MEM; Gibco; Thermo Fisher Scientific, Inc.). Cells were cultured at 37°C in 5% CO₂. Cells were seeded at a concentration of 5x10⁵ cells/well in 6 well plates. The plasmids were mixed in a 1.5 ml Eppendorf tube with 1.5 μ g Lentiviruses plus 1.5 μ g packing vector (pLVX-Puro-TSG-6; pHelper 1.0; pHelper 2.0=5:3:2) and 125 μ l MEM medium, then 5 μ l Lipo in 125 μ l MEM added. The Lipo and plasmids mixture was mixed and incubated for 20 min at 25°C. During the incubation of the Lipo and plasmids mixture, the culture medium of the 293T cells was replaced with fresh MEM medium. Then the transfection mixture was added to the well, and it was moved to an incubator at 37°C and 5% CO₂. At 8 h following transfection, the medium was replaced with fresh growth medium. After culture for 48 h, the supernatant containing lentivirus particles was collected and centrifuged at 1,258 x g for 5 min, and cell debris was discarded. In order to obtain a high concentration of lentivirus, the supernatant was further filtered to remove cells and debris. The virus titer in 293T cells was determined by end-point dilution assay.

Infection with recombinant lentiviruses. KFs in logarithmic growth phase were divided into three groups: pLVX-Puro-TSG-6 group, pLVX-Puro group and KFs group. In each group, 8x10⁴ cells were seeded into a 6-well plate and cultured in an incubator with 5% CO₂ at 37°C for 24 h. Following adhesion, the supernatant was discarded, and 2 ml DMEM containing 10% fetal calf serum (Gibco; Thermo Fisher Scientific, Inc.) was added. Once the cells reached 30% confluence, the medium was removed. Subsequently, pLVX-Puro-TSG-6 or pLVX-Puro were added into the wells at multiplicity of infection of 10. Following the addition of 50 μ l polybrene, DMEM containing 10% fetal calf serum was added to reach a total of 2 ml. For the KF group (2 wells), only 2 ml DMEM containing 10% fetal calf

Table I. Patient information.

Patient number	Sex	Age	Position	Cause of scar
01	Male	03	Anterior neck	Scald
02	Female	05	Chest	Scald
03	Female	06	Shoulder	Burn
04	Female	09	Back	Surgery
05	Male	14	Chest	Burn
06	Female	18	Earlobe	Puncture
07	Female	19	Earlobe	Puncture
08	Male	23	Upper Arm	Surgery
09	Female	25	Abdomen	Surgery
10	Female	27	Earlobe	Puncture

serum was added. Stable transfectants of pLVX-Puro-TSG-6 and pLVX-Puro were continuously selected using 2.5 μ g/ml puromycin. Stable transfection was further confirmed by reverse transcription-PCR (RT-PCR) and western blot analysis.

RNA isolation and RT-PCR. Levels of specific mRNAs in each group were assessed by RT-PCR. Total RNA was extracted using the Trizol reagent (Invitrogen; Thermo Fisher Scientific, Inc.). Purified RNA (1 μ g) was reverse transcribed using the RNA PCR Kit (Takara Biotechnology Co., Ltd., Dalian, China) according to the manufacturer's protocol. PCR primers are listed in Table II. cDNA was amplified and quantified using the RT-PCR Kit and the following conditions: 94°C for 5 min, then 40 cycles consisting of 30 sec at 94°C, 30 sec at 54°C and 45 sec at 72°C, followed by incubation at 72°C for 10 min.

PCR products with UltraPure Ethidium bromide (EB; Invitrogen, Thermo Fisher Scientific, Inc.) were electrophoresed on a 2% agarose gel. An image of the gel was captured and the intensity of the bands was analyzed using Labworks software (UVP; LLC, Phoenix, AZ, USA). β -actin was used as the internal loading control.

Western blot analysis. Total protein was prepared using RIPA Lysis and Extraction Buffer (Thermo Fisher Scientific, Inc.) at freezing temperature (Cell Signaling Technology, Inc., Danvers, MA, USA). Protein concentration was measured using a bicinchoninic acid assay protein concentration kit (Pierce; Thermo Fisher Scientific, Inc.). Equal amounts of cell lysate (50 μ g of protein) were boiled for 5 min and resolved by SDS-PAGE (12%), then electrophoretically transferred onto a nitro-cellulose membrane. The membrane was blocked with 5% non-fat dry milk in Tris-buffered saline with Tween (TBST) overnight at 4°C, then incubated with appropriate primary antibodies: TSG-6 (cat. no. ab128266; Abcam, Cambridge, MA, USA; 1:1,000); p21 (cat. no. 2947; Cell Signaling Technology, Inc.; 1:1,000); cyclin D1 (cat. no. 2978; Cell Signaling Technology, Inc.; 1:1,000); apoptosis regulator Bcl-2-associated X protein (Bax; cat. no. 5023; Cell Signaling Technology, Inc.; 1:1,000); apoptosis regulator B-cell lymphoma-2 (Bcl-2; cat. no. 2872; Cell Signaling Technology, Inc.; 1:1,000); caspase-3 (cat. no. 9662; Cell Signaling Technology, Inc.; 1:1,000); nuclear

Table II. Oligonucleotides used in reverse-polymerase chain reaction analysis.

Gene	Forward (5'-3')	Reverse (5'-3')
p21	CGTGAGCGATGGAACCTTCGA	CTCTTGGAGAAGATCAGCCG
Cyclin D1	CCCTCGGTGTCCTACTTCA	CTCCTCGCACTTCTGTTCCT
Bax	GACGGCCTCCTCTCCTACTT	CTCAGCCCATCTTCTTCCAG
Bcl-2	GAAGTGGGGGAGGATTGTGG	CCGTACAGTTCCACAAAGGC
Caspase-3	TGGAATTGATGCGTGATGTT	GTCGGCATACTGTTTCAGCA
NF-κB	AAGATCAATGGCTACACAGG	CCTCAATGTCCTCTTTCTGC
β-actin	CTCCATCCTGGCCTCGCTGT	GCTGTACCTTCACCGTTCC

Bax, apoptosis regulator Bcl-2-associated X protein; Bcl-2, apoptosis regulator B-cell lymphoma-2; NF-κB, nuclear factor-κB.

factor-κB (NF-κB; cat. no. 8242; Cell Signaling Technology, Inc.; 1:1,000); GAPDH (cat. no. 5174; Cell Signaling Technology, Inc.; 1:1,000); β-actin (cat. no. 4970; Cell Signaling Technology, Inc.; 1:1,000) in blocking buffer for 2 h at room temperature or 8-12 h at 4°C. Following washing with TBST, the membranes were then incubated with appropriate secondary antibody (goat anti-rabbit; cat. no. 7074; Cell Signaling Technology, Inc.; 1:10,000) for 3 h at room temperature. After washing with TBST, proteins were visualized using an enhanced chemiluminescence assay kit (Thermo Fisher Scientific, Inc.). Grey scale scanning was used to analyze relative expression by using Quantity One 1D Analysis software (version 4.4, Bio-Rad Laboratories, Inc., Hercules, CA, USA).

MTT assay. An MTT assay was performed to evaluate cell proliferation of pLVX-Puro-TSG-6 transfected cells, pLVX-Puro transfected cells and KFs. Single-cell suspensions (1x10⁵ cells/ml) were prepared for each group, and 100 μl cell suspension was seeded into 96-well plates and incubated at 37°C with 5% CO₂ to form a monolayer. At 24 h, once cells had adhered, 10 μl MTT stock solution (Promega Corporation, Madison, WI, USA) was added to each well, and the plate was then incubated at 37°C for 4 h. The MTT stock solution was discarded and 10 μl MTT solvent was added to each well and incubated for 4 h at 37°C to allow the crystals to be fully dissolved. The OD values at 570 nm were determined and the experiment was repeated three times. Assay was also performed at 48, 72, 96 and 120 h after plating.

Flow cytometry assay. Flow cytometry was performed to evaluate apoptosis and cell cycle arrest of the pLVX-Puro-TSG-6 transfected cells, pLVX-Puro transfected cells and KFs. Cells in each group were collected, digested with trypsin, washed with PBS three times, and centrifuged at 4°C for 5 min at 560 x g, and the supernatant was discarded. The cells were fixed with 70% ethanol at 4°C for ≥24 h and then washed with PBS twice, following removal of ethanol by centrifugation. Cell apoptosis was detected using Annexin V-FITC Apoptosis Staining/Detection kit (Abcam). Cells (1x10⁵) were collected by centrifugation 4°C for 5 min at 560 x g and re-suspended in 500 μl 1X binding buffer. Following incubation with 5 μl of Annexin V-fluorescein isothiocyanate (FITC) and 5 μl of propidium iodide (PI), the cells were maintained at room temperature for 5 min in the dark. Apoptosis was detected

using a flow cytometer and analyzed with FlowJo 10.0.6 (FlowJo LLC, Ashland, OR, USA).

For cell cycle analysis, cells from each group were fixed in 70% ethanol for 1-3 h at 4°C. After washing with PBS, cells were collected with RNase A and stained with PI for 15 min at 37°C. Cell cycle was analyzed with the flow cytometer, and the distribution of all cell-cycle phases was determining with Modfit Software (BD Biosciences, Franklin Lakes, NJ, USA).

Statistical analysis. All data are presented as the mean ± standard deviation. Statistical analysis was performed using SPSS 17.0 software (SPSS, Inc., Chicago, IL, USA). Tests for homogeneity of variance (Levene's test) and one-way analysis of variance procedures were performed, and followed by Turkey's multiple comparison post hoc test. P<0.05 was considered to indicate a statistically significant difference.

Results

Transfection efficiency. An 828 bp target gene fragment was obtained from agarose gel electrophoresis of a PCR product, the size of which was in accordance with TSG-6. The results suggested that TSG-6 gene was successfully cloned into the pLVX-Puro vector (Fig. 1). Agarose gel electrophoresis revealed the positive clones after infection, with 1,179 bp and 198 bp size bands for positive and negative transformants, respectively (Fig. 2). After BLAST detection, the sequencing results of the clones revealed that the sequence identity was 828/828 (100%) and the target gene lentiviral vector had been successfully constructed (Fig. 3).

TSG-6 expression in KFs following infection. To determine the efficiency of transfection in KFs, total RNA was extracted and RT-PCR was performed. The data indicated that a high level of TSG-6 mRNA expression was detected in the pLVX-Puro-TSG-6 group compared with the KF and Plvx-Puro groups (P<0.05), while there was no significant difference between the pLVX-Puro group and the KF group (P>0.05). This suggested that the exogenous TSG-6 gene was transduced successfully (Fig. 4). To further verify this result, TSG-6 protein expression was determined using western blot analysis. The results suggested that the expression of TSG-6 protein was increased significantly in the pLVX-Puro-TSG-6

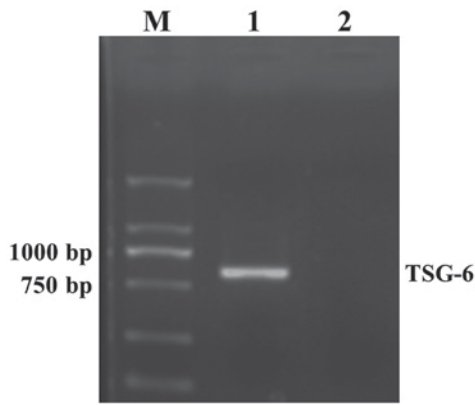


Figure 1. Agarose gel electrophoresis of TSG-6 gene clone. TSG-6, tumor necrosis factor-stimulated gene-6.

group compared with the pLVX-Puro group and the KF group ($P < 0.05$), while there was no significant difference between the pLVX-Puro group and the KF group ($P > 0.05$; Fig. 5).

TSG-6 overexpression inhibited cell proliferation. Cell viability was determined using an MTT assay. Compared with the control and pLVX-Puro group, the proliferation of the TSG-6 transfected cells was significantly decreased. However, there was no significant difference between the pLVX-Puro group and the KF group, which demonstrated that the vector itself had no effect on the viability of KFs (Fig. 6).

Overexpression of TSG-6 induced apoptosis of KFs. Flow cytometry was performed to determine the rate of cell apoptosis. Apoptosis was analyzed by double-staining with Annexin V-FITC and PI. The apoptosis rate in the pLVX-Puro-TSG-6 group was 51.92%, which was significantly higher than that in pLVX-Puro group (19.00%) and the KF group (3.59%; $P < 0.05$). There was no significant difference in apoptosis rate between the pLVX-Puro group and the KF cell group (Fig. 7).

TSG-6 regulated expression of genes and proteins involved in proliferation, cell cycle and apoptosis. Whether the regulation of TSG-6 affects proteins involved in proliferation, apoptosis and cell cycle in KFs was investigated. Total cellular

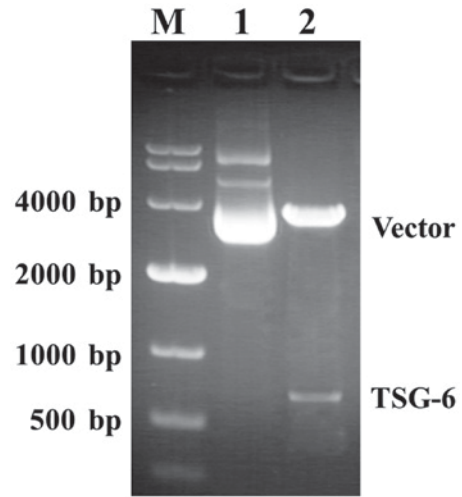


Figure 2. Agarose gel electrophoresis of the digested product from vector. M, marker; 1, pLVX-Puro vector; 2, pLVX-Puro-TSG-6 vector; TSG-6, tumor necrosis factor-stimulated gene-6.

mRNA or protein was isolated from cells transfected with pLVX-Puro-TSG-6 or pLVX-Puro, and untransfected cells. Flow cytometry analysis suggested that cells were arrested in G2/M phase by TSG-6 overexpression (Fig. 8). Levels of p21, cyclin D1, Bax, Bcl-2, caspase-3 and NF- κ B were determined by RT-PCR and western blot. The RT-PCR results indicated that transfection of TSG-6 led to an increase in the expression of p21, Bax and caspase-3. Additionally, overexpression of TSG-6 decreased the mRNA levels of cyclin D1 and NF- κ B (Fig. 9). The ratio of Bcl-2/Bax was also decreased significantly in the TSG-6-transfected cells compared with the control group. Similar results were confirmed by western blot; overexpressed TSG-6 markedly increased the protein levels of p21, Bax and caspase-3 (Fig. 10).

Discussion

Keloid formation occurs when the normal wound-healing process is disordered and the evolving scar remains in the proliferative phase of healing. The scar may grow beyond the boundaries of the original wound (13). It has been identified

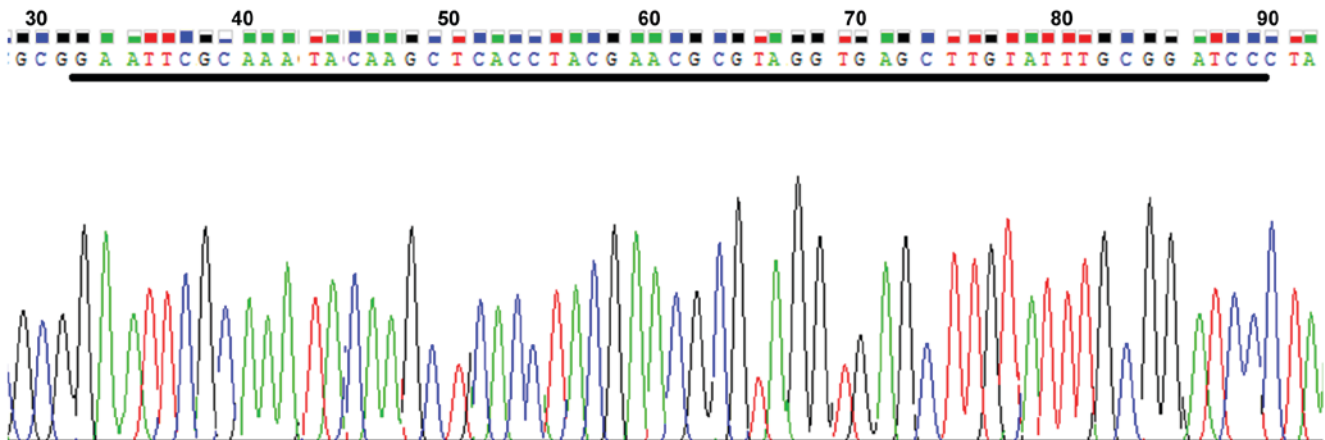


Figure 3. Sequencing of the clone fragment inserted into the plasmid vector.

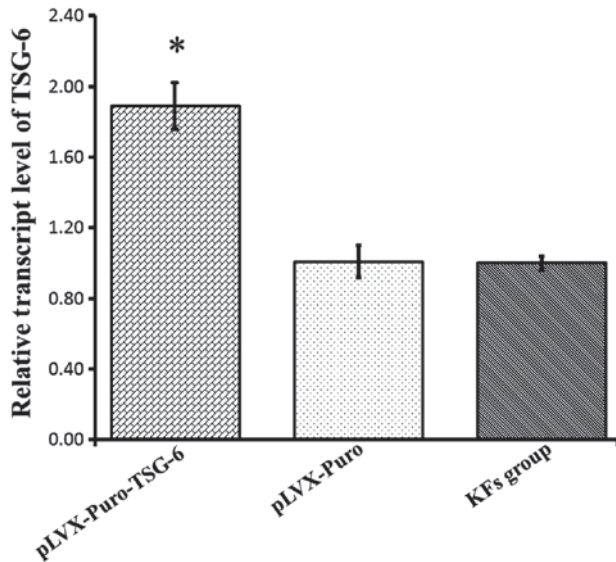


Figure 4. TSG-6 mRNA expression in each group. Data are presented as mean \pm standard deviation. * $P < 0.05$ vs. KFs. TSG-6, tumor necrosis factor-stimulated gene-6; KFs, keloid fibroblasts.

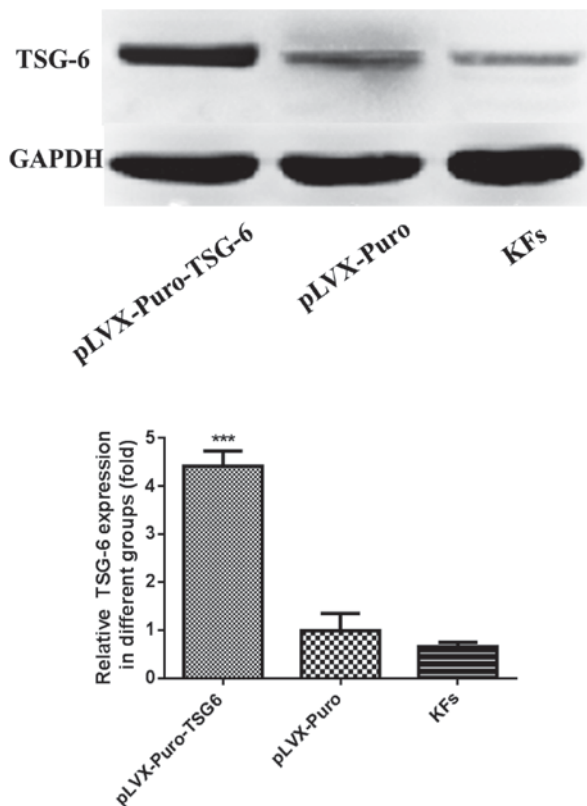


Figure 5. Expression of TSG-6 protein in each group. Data are presented as mean \pm standard deviation. *** $P < 0.05$ vs. KFs. TSG-6, tumor necrosis factor-stimulated gene-6; KFs, keloid fibroblasts.

that apoptosis may be a mechanism by which granulation tissue develops, thus decreasing cellularity and scar formation (14). The mRNA expression of TSG-6 in keloid was previously compared with normal skin and it was demonstrated that low expression of TSG-6 may participate in the formation of keloid. The previous investigations indicated that

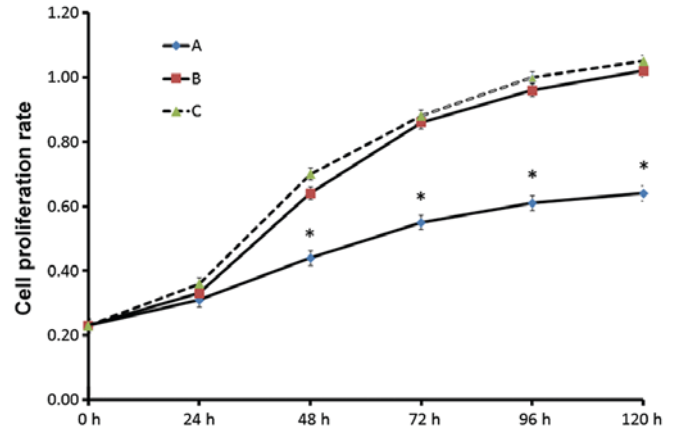


Figure 6. Effect of TSG-6 on cell proliferation in each group. A, pLVX-Puro-TSG-6 transfected cells; B, pLVX-Puro transfected cells; C, keloid fibroblasts. Data are presented as mean \pm standard deviation. * $P < 0.05$ vs. KFs. TSG-6, tumor necrosis factor-stimulated gene-6.

the expression level of TSG-6 in primary keloid fibroblasts derived from individual patients was significantly higher than in normal skin (15), which is supported by the results and conclusions of the present study.

TSG-6 is a hyaluronic acid (HA)-binding protein composed of a single-strand module of two α -helices and two triple-strand β -sheets arranged around a large hydrophobic core (16). TSG-6 is involved in the regulation of leukocyte migration and the pattern of expression indicates that it may be associated with extracellular matrix remodeling (17). Increased TSG-6 protein expression has been detected in the synovial fluid of patients with arthritis, and recombinant TSG-6 protein has been identified to have potent anti-inflammatory effects *in vivo* (18). It has been indicated that TSG-6 is part of a cytokine-initiated feedback loop that reduces the inflammatory response. TSG-6 was observed to form a stable, possibly covalent, 120 kDa complex with a serine protease inhibitor and inter- α inhibitor (I α I) (19). Furthermore, anti-plasmin activity was significantly increased by this complex compared with I α I alone (20). In conclusion, TSG-6 may be a key factor involved in regulating leukocyte migration and matrix remodeling, caused by break down of latent metalloproteinases in the extracellular matrix via enhanced activity of plasmin.

In the current study, a lentiviral vector carrying the TSG-6 gene was transfected into KFs, and increased the expression of TSG-6 mRNA confirmed that the transduction was effective. In addition, western blot results indicated that the TSG-6 protein in the pLVX-Puro-TSG-6 group was primarily encoded by the exogenous TSG-6 gene. To determine whether TSG-6 has selective cytotoxic activity in KFs, MTT and apoptosis assays were performed, and the mRNA and protein levels of key molecules were determined. According to the MTT results, TSG-6 inhibited KF proliferation selectively compared with the negative control. Flow cytometry analysis suggested that TSG-6 selectively induced KF cell death and accumulation of cells in G2/M phase by preventing KFs from entering M phase. RT-PCR and western blot results also supported these conclusions.

Recent studies have revealed that keloids have tumor-like biological functions, and the roles of therapeutic strategies such as microRNAs, bone morphogenetic proteins, activin

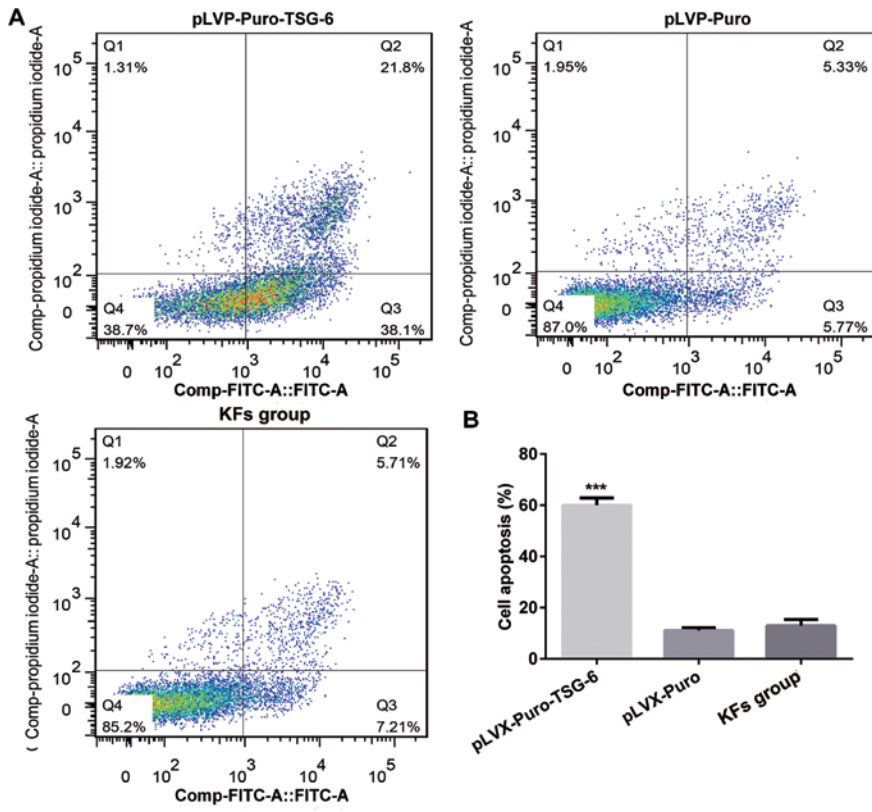


Figure 7. Effect of TSG-6 on apoptosis in each group. (A) Apoptosis analysis of pLVX-Puro-TSG-6 transfected cells, pLVX-Puro transfected cells and KFs via flow cytometry. (B) Apoptosis quantification. All data are presented as the mean \pm standard deviation. Data are presented as mean \pm standard deviation. ***P<0.05 vs. KFs. TSG-6, tumor necrosis factor-stimulated gene-6; KFs, keloid fibroblasts.

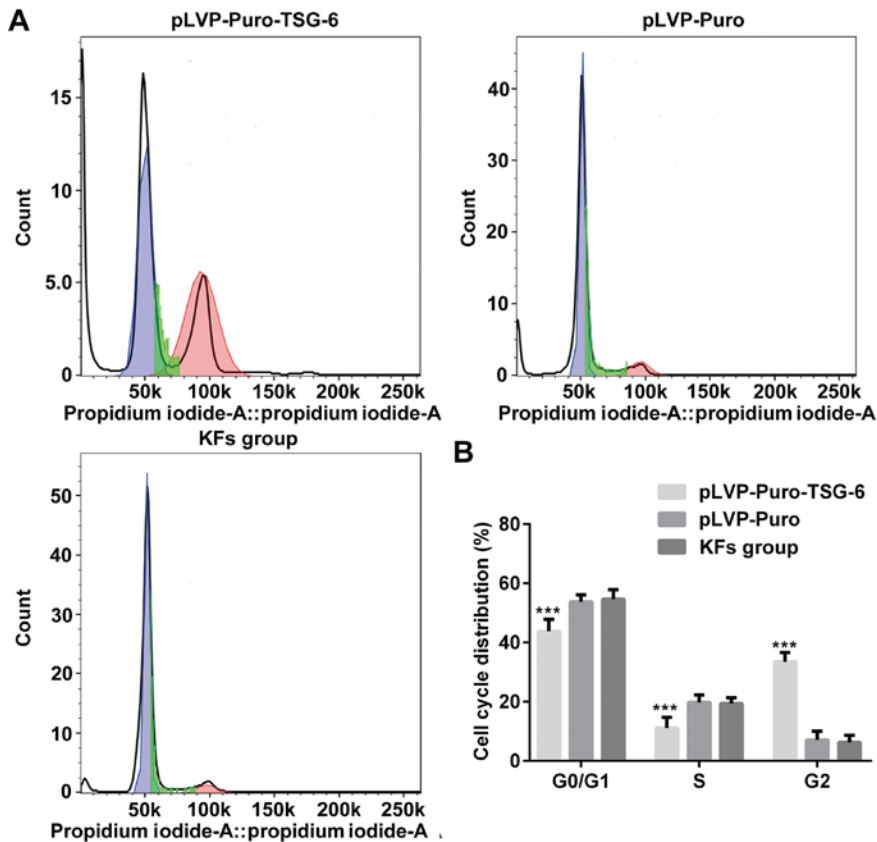


Figure 8. Effect of TSG-6 on cell cycle in each group. (A) Cell cycle analysis of pLVX-Puro-TSG-6 transfected cells, pLVX-Puro transfected cells and KFs via flow cytometry. (B) Cell cycle distribution quantification. All data are presented as the mean \pm standard deviation. Data are presented as mean \pm standard deviation. ***P<0.05 vs. KFs. TSG-6, tumor necrosis factor-stimulated gene-6; KFs, keloid fibroblasts.

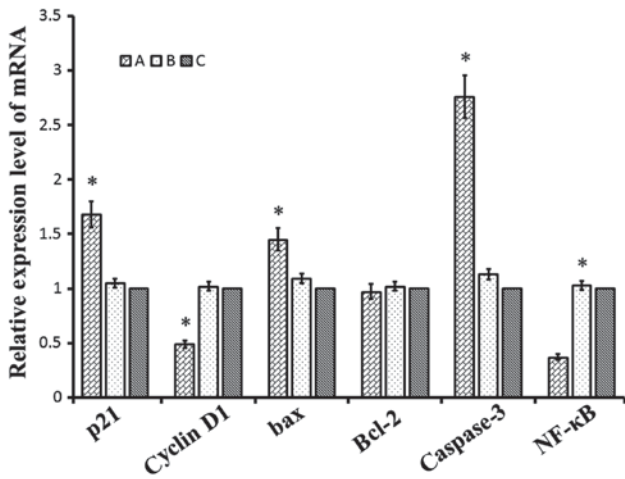


Figure 9. Relative mRNA expression levels of p21, cyclin D1, Bax, Bcl-2, caspase-3 and NF-κB. A, pLVX-Puro-TSG-6 transfected cells; B, pLVX-Puro transfected cells; C, keloid fibroblasts. Data were presented by mean ± SD. *P<0.05 vs. KFs. TSG-6, tumor necrosis factor-stimulated gene-6; Bax, apoptosis regulator Bcl-2-associated X protein; Bcl-2, apoptosis regulator B-cell lymphoma-2; NF-κB, nuclear factor-κB.

membrane bound inhibitor and heat shock protein 70 in keloids have been investigated (21-23). It has been confirmed that TSG-6 is lowly expressed in prostate cancer and can be a potential marker for prostate cancer diagnosis (24). A previous study identified that TSG-6 combined with Yeast Cytosine Deaminase and 5-Fluorocytosine exerts anti-tumor effects (25). Pathogenic mechanisms of keloid have not been elucidated in detail; however, controlling fibroblast proliferation and apoptosis via certain targeted genes may be an effective therapeutic strategy for treating keloids. In the current study, TSG-6 overexpression increased apoptosis and decreased cell proliferation, which could offer a protective effect against keloid development.

In summary, KFs transfected with a lentiviral vector carrying TSG-6 expressed a high level of exogenous TSG-6. Transduction of the pLVX-Puro-TSG-6 selectively suppressed proliferation and induced apoptosis in KFs, which confirmed the role of TSG-6 in KFs. As a result, TSG-6 has potential as a gene therapy candidate for the treatment of keloid, and may result in novel and effective therapeutic approaches.

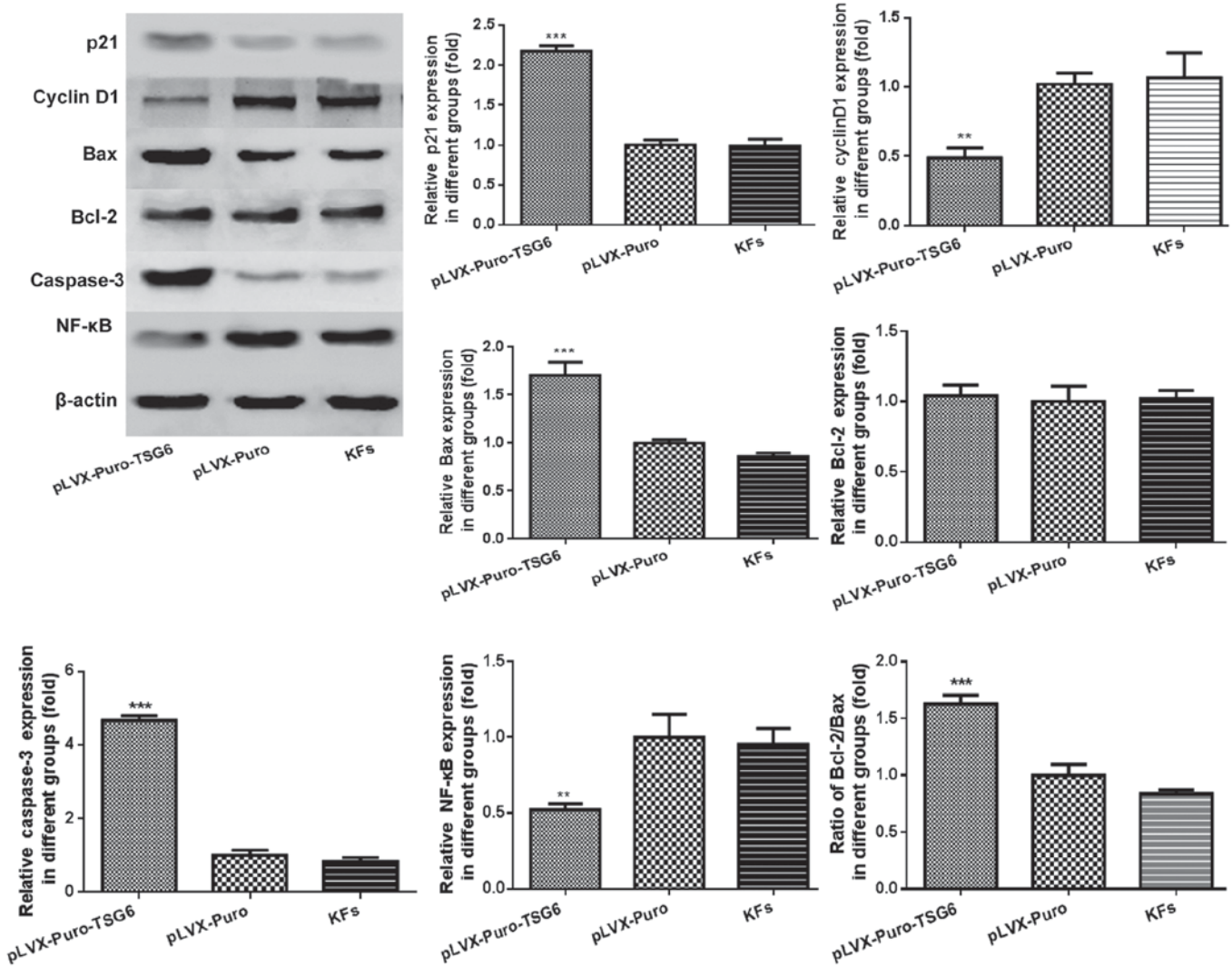


Figure 10. Protein expression of p21, cyclin D1, Bax, Bcl-2, caspase-3 and NF-κB. Data are presented as mean ± standard deviation. **P<0.05, ***P<0.05 vs. KFs. Bax, apoptosis regulator Bcl-2-associated X protein; Bcl-2, apoptosis regulator B-cell lymphoma-2; NF-κB, nuclear factor-κB; TSG-6, tumor necrosis factor-stimulated gene-6; KFs, keloid fibroblasts.

Acknowledgements

Not applicable.

Funding

This work was supported by the National Natural Science Foundation of China (no. 81272107).

Availability of data and materials

The datasets used and/or analyzed during the current study are available from the corresponding author on reasonable request.

Authors' contributions

ZC conceived, designed, coordinated and performed all the experiments, conducted the statistical analysis and drafted the manuscript. XYL collected all samples and achieved particle analysis. HW and XJL assisted in study design and manuscript editing. All the authors read and approved the final manuscript.

Ethics approval and consent to participate

The current study was approved by the institutional review board of Anhui Medical University (Hefei, China), and written informed consent was obtained from all patients prior to inclusion. The study was performed according to the principles of the Declaration of Helsinki.

Patient consent for publication

Not applicable.

Competing interests

The authors declare that they have no competing interests.

References

- Gupta J, Gantyal SP, Kashyap S and Tandon R: Diagnosis, management, and histopathological characteristics of corneal keloid: A case series and literature review. *Asia Pac J Ophthalmol (Phila)* 5: 354-359, 2016.
- Jeon YR, Ahn HM, Choi IK, Yun CO, Rah DK, Lew DH and Lee WJ: Hepatocyte growth factor-expressing adenovirus upregulates matrix metalloproteinase-1 expression in keloid fibroblasts. *Int J Dermatol* 55: 356-361, 2016.
- Syed F, Singh S and Bayat A: Superior effect of combination vs. single steroid therapy in keloid disease: A comparative in vitro analysis of glucocorticoids. *Wound Repair Regen* 21: 88-102, 2013.
- Har-Shai Y and Zouboulis CC: Intralesional cryotherapy for the treatment of keloid scars: A prospective study. *Plast Reconstr Surg* 136: 397e-398e, 2015.
- Lee MJ, Kim DH, Ryu JS, Ko AY, Ko JH, Kim MK, Wee WR, Khwang SI and Oh JY: Topical TSG-6 administration protects the ocular surface in two mouse models of inflammation-related dry eye. *Invest Ophthalmol Vis Sci* 56: 5175-5181, 2015.
- Kim JA, Ko JH, Ko AY, Lee HJ, Kim MK, Wee WR, Lee RH, Fulcher SF and Oh JY: TSG-6 protects corneal endothelium from transcorneal cryoinjury in rabbits. *Invest Ophthalmol Vis Sci* 55: 4905-4912, 2014.
- Baranova NS, Nilebäck E, Haller FM, Briggs DC, Svedhem S, Day AJ and Richter RP: The inflammation-associated protein TSG-6 cross-links hyaluronan via hyaluronan-induced TSG-6 oligomers. *J Biol Chem* 286: 25675-25686, 2011.
- Tan KT, McGrouther DA, Day AJ, Milner CM and Bayat A: Characterization of hyaluronan and TSG-6 in skin scarring: Differential distribution in keloid scars, normal scars and unscarred skin. *J Eur Acad Dermatol Venereol* 25: 317-327, 2011.
- Mahoney DJ, Swales C, Athanasou NA, Bombardieri M, Pitzalis C, Kliskey K, Sharif M, Day AJ, Milner CM and Sabokbar A: TSG-6 inhibits osteoclast activity via an autocrine mechanism and is functionally synergistic with osteoprotegerin. *Arthritis Rheum* 63: 1034-1043, 2011.
- Kehlen A, Pachnio A, Thiele K and Langner J: Gene expression induced by interleukin-17 in fibroblast-like synoviocytes of patients with rheumatoid arthritis: Upregulation of hyaluronan-binding protein TSG-6. *Arthritis Res Ther* 5: R186-R192, 2003.
- Wang H, Chen Z, Li XJ, Ma L and Tang YL: Anti-inflammatory cytokine TSG-6 inhibits hypertrophic scar formation in a rabbit ear model. *Eur J Pharmacol* 751: 42-49, 2015.
- Zhang GY, Yi CG, Li X, Zheng Y, Niu ZG, Xia W, Meng Z, Meng CY and Guo SZ: Inhibition of vascular endothelial growth factor expression in keloid fibroblasts by vector-mediated vascular endothelial growth factor shRNA: A therapeutic potential strategy for keloid. *Arch Dermatol Res* 300: 177-184, 2008.
- Hochman B, Isoldi FC, Furtado F and Ferreira LM: New approach to the understanding of keloid: Psychoneuroimmune-endocrine aspects. *Clin Cosmet Investig Dermatol* 8: 67-73, 2015.
- Parikh DA, Ridgway JM and Ge NN: Keloid banding using suture ligation: A novel technique and review of literature. *Laryngoscope* 118: 1960-1965, 2008.
- Hong X, Li X and Ning J: Expression of TSG-6 and its significance in pathological scar. *Acta Univ Med Anhui* 48: 685-687, 2013 (In Chinese).
- Milner CM, Higman VA and Day AJ: TSG-6: A pluripotent inflammatory mediator? *Biochem Soc Trans* 34: 446-450, 2006.
- Park Y, Jowitt TA, Day AJ and Prestegard JH: Nuclear magnetic resonance insight into the multiple glycosaminoglycan binding modes of the link module from human TSG-6. *Biochemistry* 55: 262-276, 2016.
- Nagyeri G, Radacs M, Ghassemi-Nejad S, Tryniszewska B, Olasz K, Hutas G, Gyorffy Z, Hascall VC, Glant TT and Mikecz K: TSG-6 protein, a negative regulator of inflammatory arthritis, forms a ternary complex with murine mast cell tryptases and heparin. *J Biol Chem* 286: 23559-23569, 2011.
- Baranova NS, Foulcer SJ, Briggs DC, Tilakaratna V, Enghild JJ, Milner CM, Day AJ and Richter RP: Inter- α -inhibitor impairs TSG-6-induced hyaluronan cross-linking. *J Biol Chem* 288: 29642-29653, 2013.
- Zhang S, He H, Day AJ and Tseng SC: Constitutive expression of inter- α -inhibitor (I α) family proteins and tumor necrosis factor-stimulated gene-6 (TSG-6) by human amniotic membrane epithelial and stromal cells supporting formation of the heavy chain-hyaluronan (HC-HA) complex. *J Biol Chem* 287: 12433-12444, 2012.
- Zhang GY, Wu LC, Liao T, Chen GC, Chen YH, Zhao YX, Chen SY, Wang AY, Lin K, Lin DM, *et al.*: A novel regulatory function for miR-29a in keloid fibrogenesis. *Clin Exp Dermatol* 41: 341-345, 2016.
- Lin L, Wang Y, Liu W and Huang Y: BAMBI inhibits skin fibrosis in keloid through suppressing TGF- β 1-induced hyperplastic fibroblast cell proliferation and excessive accumulation of collagen I. *Int J Clin Exp Med* 8: 13227-13234, 2015.
- Shin JU, Lee WJ, Tran TN, Jung I and Lee JH: Hsp70 knockdown by siRNA decreased collagen production in keloid fibroblasts. *Yonsei Med J* 56: 1619-1626, 2015.
- Garcia GE, Wisniewski HG, Lucia MS, Arevalo N, Slaga TJ, Kraft SL, Strange R and Kumar AP: 2-Methoxyestradiol inhibits prostate tumor development in transgenic adenocarcinoma of mouse prostate: Role of tumor necrosis factor- α -stimulated gene 6. *Clin Cancer Res* 12: 980-988, 2006.
- Park JI, Cao L, Platt VM, Huang Z, Stull RA, Dy EE, Sperinde JJ, Yokoyama JS and Szoka FC: Antitumor therapy mediated by 5-fluorocytosine and a recombinant fusion protein containing TSG-6 hyaluronan binding domain and yeast cytosine deaminase. *Mol Pharm* 6: 801-812, 2009.



This work is licensed under a Creative Commons Attribution-NonCommercial-NoDerivatives 4.0 International (CC BY-NC-ND 4.0) License.